

REPORT DOCUMENTATION PAGE			Form Approved OMB NO. 0704-0188		
<p>The public reporting burden for this collection of information is estimated to average 1 hour per response, including the time for reviewing instructions, searching existing data sources, gathering and maintaining the data needed, and completing and reviewing the collection of information. Send comments regarding this burden estimate or any other aspect of this collection of information, including suggestions for reducing this burden, to Washington Headquarters Services, Directorate for Information Operations and Reports, 1215 Jefferson Davis Highway, Suite 1204, Arlington VA, 22202-4302. Respondents should be aware that notwithstanding any other provision of law, no person shall be subject to any penalty for failing to comply with a collection of information if it does not display a currently valid OMB control number.</p> <p>PLEASE DO NOT RETURN YOUR FORM TO THE ABOVE ADDRESS.</p>					
1. REPORT DATE (DD-MM-YYYY)		2. REPORT TYPE New Reprint		3. DATES COVERED (From - To) -	
4. TITLE AND SUBTITLE Preparation and characterization of an alkaline anion exchange membrane from chlorinated poly(propylene) aminated with branched poly(ethyleneimine)			5a. CONTRACT NUMBER W911NF-10-1-0520		
			5b. GRANT NUMBER		
			5c. PROGRAM ELEMENT NUMBER 611103		
6. AUTHORS Ashley M. Maes, Tara P. Pandey, Melissa A. Vandiver, Lauren K. Lundquist, Yuan Yang, James L. Horan, Anastasia Krosovsky, Matthew W. Liberatore, Sönke Seifert, Andrew M. Herring			5d. PROJECT NUMBER		
			5e. TASK NUMBER		
			5f. WORK UNIT NUMBER		
7. PERFORMING ORGANIZATION NAMES AND ADDRESSES Colorado School of Mines Research Administration 1500 Illinois St Golden, CO 80401 -1911				8. PERFORMING ORGANIZATION REPORT NUMBER	
9. SPONSORING/MONITORING AGENCY NAME(S) AND ADDRESS(ES) U.S. Army Research Office P.O. Box 12211 Research Triangle Park, NC 27709-2211				10. SPONSOR/MONITOR'S ACRONYM(S) ARO	
				11. SPONSOR/MONITOR'S REPORT NUMBER(S) 58161-CH-MUR.41	
12. DISTRIBUTION AVAILABILITY STATEMENT Approved for public release; distribution is unlimited.					
13. SUPPLEMENTARY NOTES The views, opinions and/or findings contained in this report are those of the author(s) and should not be construed as an official Department of the Army position, policy or decision, unless so designated by other documentation.					
14. ABSTRACT A new randomly crosslinked polymer is investigated for use as an ion-exchange membrane. The polymer was produced through amination of chlorinated poly(propylene) (PP) with poly(ethyleneimine) (PEI) and quaternized with iodoethane. The synthesis of the new polymer is confirmed by FTIR 1 H and 13 C NMR. The microstructure of the polymer consists of aggregates on the order of 1 micrometer. Environmentally controlled small and wide angle X-ray analysis showed a relatively featureless amorphous morphology over length scales less than 105 nm					
15. SUBJECT TERMS Anion exchange membrane, Fuel Cell, Poly(ethyleneimine), Quaternary ammonium cation, Hydroxide					
16. SECURITY CLASSIFICATION OF:			17. LIMITATION OF ABSTRACT UU	18. NUMBER OF PAGES	19a. NAME OF RESPONSIBLE PERSON Andrew Herring
a. REPORT UU	b. ABSTRACT UU	c. THIS PAGE UU			19b. TELEPHONE NUMBER 303-384-2082

## Report Title

Preparation and characterization of an alkaline anion exchange membrane from chlorinated poly(propylene) aminated with branched poly(ethyleneimine)

### ABSTRACT

A new randomly crosslinked polymer is investigated for use as an ion-exchange membrane. The polymer was produced through amination of chlorinated poly(propylene) (PP) with poly(ethyleneimine) (PEI) and quaternized with iodoethane. The synthesis of the new polymer is confirmed by FTIR  $^1\text{H}$  and  $^{13}\text{C}$  NMR. The microstructure of the polymer consists of aggregates on the order of 1 micrometer. Environmentally controlled small and wide angle X-ray analysis showed a relatively featureless amorphous morphology over length scales less than 105 nm through a full range of humidity environments. Little physical swelling of the films were observed, but very high internal water uptake was observed with  $\lambda = 50$ . The highest in-plane ionic conductivity with chloride as the counter ion observed was  $0.29\text{ mS cm}^{-1}$  at  $90^\circ\text{C}$  and 95% relative humidity. Infrared spectroscopy was used to monitor the relatively rapid rate of counter-ion reaction of hydroxide with ambient  $\text{CO}_2$  to form a mixture of carbonate and bicarbonate when exposed to air.

---

**REPORT DOCUMENTATION PAGE (SF298)**  
**(Continuation Sheet)**

---

Continuation for Block 13

ARO Report Number    58161.41-CH-MUR  
Preparation and characterization of an alkaline a    ...

Block 13: Supplementary Note

© 2013 . Published in Electrochimica Acta, Vol. Ed. 0 (2013), (Ed. ). DoD Components reserve a royalty-free, nonexclusive and irrevocable right to reproduce, publish, or otherwise use the work for Federal purposes, and to authorize others to do so (DODGARS §32.36). The views, opinions and/or findings contained in this report are those of the author(s) and should not be construed as an official Department of the Army position, policy or decision, unless so designated by other documentation.

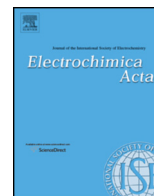
Approved for public release; distribution is unlimited.



Contents lists available at SciVerse ScienceDirect

Electrochimica Acta

journal homepage: [www.elsevier.com/locate/electacta](http://www.elsevier.com/locate/electacta)



## Preparation and characterization of an alkaline anion exchange membrane from chlorinated poly(propylene) aminated with branched poly(ethyleneimine)

Ashley M. Maes<sup>a</sup>, Tara P. Pandey<sup>a</sup>, Melissa A. Vandiver<sup>a</sup>, Lauren K. Lundquist<sup>a</sup>, Yuan Yang<sup>b</sup>, James L. Horan<sup>a</sup>, Anastasia Krosovsky<sup>a</sup>, Matthew W. Liberatore<sup>a</sup>, Sönke Seifert<sup>c</sup>, Andrew M. Herring<sup>a,\*,1</sup>

<sup>a</sup> Department of Chemical and Biological Engineering, Colorado School of Mines, Golden, CO 80401, USA

<sup>b</sup> Department of Chemistry and Geochemistry, Colorado School of Mines, Golden, CO 80401, USA

<sup>c</sup> X-ray Sciences Division, Argonne National Laboratory, 9700 South Cass Avenue, Argonne, IL 60439, USA

### ARTICLE INFO

#### Article history:

Received 4 December 2012

Received in revised form 29 March 2013

Accepted 2 April 2013

Available online xxx

#### Keywords:

Anion exchange membrane

Fuel cell

Poly(ethyleneimine)

Quaternary ammonium cation

Hydroxide

### ABSTRACT

A new randomly crosslinked polymer is investigated for use as an ion-exchange membrane. The polymer was produced through amination of chlorinated poly(propylene) (PP) with poly(ethyleneimine) (PEI) and quaternized with iodoethane. The synthesis of the new polymer is confirmed by FTIR <sup>1</sup>H and <sup>13</sup>C NMR. The microstructure of the polymer consists of aggregates on the order of 1 μm. Environmentally controlled small and wide angle X-ray analysis showed a relatively featureless amorphous morphology over length scales less than 105 nm through a full range of humidity environments. Little physical swelling of the films were observed, but very high internal water uptake was observed with λ = 50. The highest in-plane ionic conductivity with chloride as the counter ion observed was 0.29 mS cm<sup>-1</sup> at 90 °C and 95% relative humidity. Infrared spectroscopy was used to monitor the relatively rapid rate of counter-ion reaction of hydroxide with ambient CO<sub>2</sub> to form a mixture of carbonate and bicarbonate when exposed to air.

© 2013 Elsevier Ltd. All rights reserved.

### 1. Introduction

Anion exchange polymers have applications as ion exchange resins and as membranes for water purification [1], Li–air batteries, and in polymer exchange membrane (PEM) fuel cells [2]. PEM Fuel cells show promise as alternatives to current energy conversion devices in transportation and stationary applications as well as for use in portable devices. There is currently a large amount of interest in using anion exchange membranes (AEMs) as the electrolyte in alkali fuel cells, because of the increased power density obtained with a solid electrolyte. AEM fuel cells (AEMFCs) have advantages over proton exchange membrane fuel cells, with the potential for direct use of methanol or more complex fuels, and the potential use of non-precious metal catalysts [2]. Commercial AEMs are available from companies such as Tokuyama [3], Solvay Plastics [4], Dupont, and Fumatech [5], although many of these materials are optimized for non-fuel cell applications such as dialysis. Commercial

membranes with acceptable mechanical properties, long-term alkaline stability and higher anionic conductivity at lower RH for fuel cell applications are still needed [6,7].

In base oxidative attack of the polymer by hydroxide is less important than degradation of the cationic functionalities [2]. It is, therefore, possible to design polymer systems with methylene chain backbones. A simple approach would be to simply react an aminated polymer with a halogenated polymer to form aminated materials that could then be readily quaternized to form a potentially inexpensive AEM. In previous work, Hong et al. have synthesized similar materials by amination of chlorinated polypropylene (CPP) with ethylenediamine (EDA) [8] and amination of PPC with low molecular weight linear PEI [9,10]. It was shown that these materials exhibit good chloride ionic conductivities in water after soaking in NaCl with a maximum of 0.008 and 0.013 S cm<sup>-1</sup> for the quaternized EDA/PPC and the quaternized PEI/PPC material respectively. To extend this group of materials, we selected a branched high molecular weight polyethyleneimine (PEI) as a starting material due to the high concentration of quaternizable amine groups throughout the polymer. Polyethyleneimine (PEI) has most commonly been investigated in biological applications where it is often crosslinked and quaternized to form stable cationic polymers. Resulting products have been shown to be

\* Corresponding author at: 1500 Illinois Street, Chemical and Biological Engineering Department, Golden, CO 80401, USA. Tel.: +1 303 384 2082.

E-mail address: [aherring@mines.edu](mailto:aherring@mines.edu) (A.M. Herring).

<sup>1</sup> ISE member.

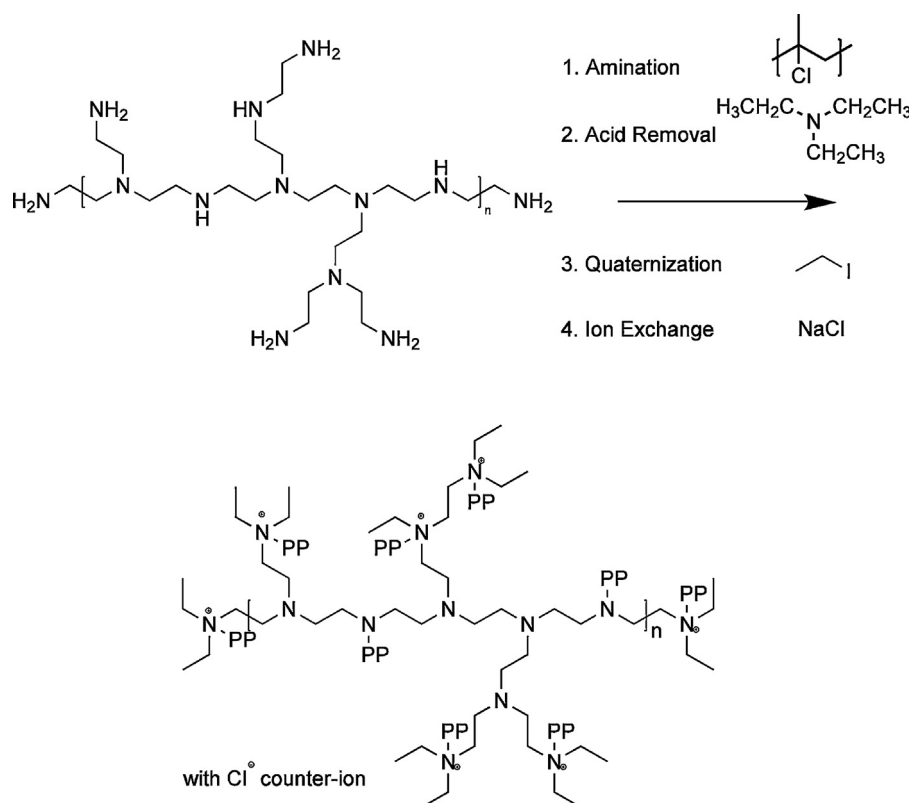
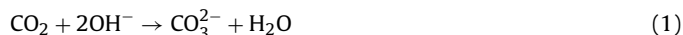


Fig. 1. Reaction sequence of quaternized PEI-PP crosslinked polymer where PP represents a chain of polypropylene.

effective in gene delivery systems and for use as antimicrobial metal surface coatings [11,12]. Its quaternized form has anti-bacterial properties [13,14].

One issue of hydroxide exchange membranes is that hydroxide reacts rapidly with the ambient CO<sub>2</sub> in the air, forming a mixture of carbonate and bicarbonate counter-ions [15]. The presence of bi(carbonate) ions in place of hydroxide ions is detrimental to the conductivity in the membrane due to inherently lower ion mobility. A reaction of a CO<sub>2</sub> molecule with a hydroxide anion in solution can produce a bicarbonate ion as shown in Eq. (1) and it may also produce a carbonate ion in the presence of two hydroxide ions as shown in Eq. (2). When CO<sub>2</sub> reacts with hydroxide ions located as counter anions in a polymeric membrane, the ratio of bicarbonates and carbonates can be determined by titration or FT-IR.



Suzuki et al. have observed these reactions of hydroxide with atmospheric CO<sub>2</sub> within the first minutes of exposure of hydroxide form Tokuyama AEMs to air [16].

Although our synthesized membrane had only a moderate IEC of 0.74(0.02) mequiv. mol<sup>-1</sup>, unique water uptake and transport were observed through Dynamic Vapor Sorption (DVS) and pulsed-field gradient nuclear magnetic resonance (PFG-NMR) spectroscopy. This paper discusses the transport of anions in the context of beginning to understand the morphology of the material. Quantitative analysis of the formation of carbonates when hydroxide counter-ions in the membrane react with atmospheric CO<sub>2</sub> is included.

## 2. Experimental

### 2.1. Materials

Branched polyethyleneimine (PEI) (solution ( $M_w \sim 2000$  by LS, 50 wt% water), chlorinated polypropylene (CPP) ( $M_w \sim 100,000$ ), trimethylamine ( $\geq 99.0\%$ ) and iodoethane (99%) were used as received (Sigma–Aldrich). All solvents were reagent grade.

### 2.2. Synthesis

In preliminary studies, branched PEI solution (50 wt% water) was quaternized with a 10-fold excess of iodoethane, under flowing nitrogen at 50 °C using a condenser to minimize evaporation. The final solution was dried in vacuo to produce a highly hygroscopic white powder.

#### 2.2.1. Quaternized PEI-polypropylene (PP-PEI)

The synthetic procedure is outlined in Fig. 1. CPP (5 g) was dissolved in toluene (50 ml) at 60 °C and added to PEI solution (10 g, 50 wt% water) at 60 °C. The amination reaction was performed at 60 °C for 48 h. The hydrochloric acid (HCl) produced during the reaction was neutralized with excess trimethylamine over 24 h. Five fold excess, based on the amine groups in the starting PEI, iodoethane was added to quaternize all the amine groups on the polymer at 60 °C for 48 h. The remaining solvent and excess trimethylamine reactants were then removed by evaporation, and the resulting polymer was washed with dionized (DI) water to extract any unreacted PEI. The resulting material was soaked in toluene, swelling considerably, and spread onto a Teflon casting block to form a membrane. The toluene was removed in vacuo at 40 °C. The resulting membrane was soaked in a 1 M NaCl solution, and again washed with DI water to guarantee that the sample was in a chloride counter-ion form for further characterization. The final

product will have quaternary ammonium groups with an unknown mix of ethyl groups and poly(propylene) chains attached to each nitrogen.

### 2.3. Characterization

#### 2.3.1. Spectroscopy

FTIR was performed using a Thermo-Nicolet 2100 FTIR spectrometer in attenuated total reflectance mode.  $^1\text{H}$ , and  $^{13}\text{C}$  magic angle spin (MAS) NMR were performed on a Bruker Avance III 400 Spectrometer with a 50 kHz B1 field. A 4 mm MAS BB/BB probe was used.  $^1\text{H}$  MAS NMR was taken at 400 MHz, with spin rates of 12 kHz with a 6 s recycle delay.  $^{13}\text{C}$  MAS NMR was recorded at 100 MHz, with a spin rate 8 kHz, a 6 s recycle delay and a 1 ms contact time.

#### 2.3.2. Ion exchange capacity

Ion exchange capacity (IEC) was measured using the Mohr titration method to determine the chloride concentration in a given sample of membrane. The sample was first dried in a vacuum oven at 40 °C overnight and weighed to determine a starting dry mass. Three samples were tested.

#### 2.3.3. Morphology

Small and wide angle X-ray scattering (SAXS and WAXS) experiments were performed at the Advanced Photon Source at Argonne National Lab on beamline 12 ID-B. A Pliatus 2M SAXS detector was used to collect scattering data with an exposure time of 1 second. The X-ray beam had a wavelength of 1 Å and power of 12 keV. The intensity ( $I$ ) is a radial integration of the 2D scattering pattern with respect to the scattering vector ( $q$ ).

Temperature and humidity were controlled during SAXS experiments within a custom built sample oven [17]. Typical experiments studied three membrane samples and one empty window so a background spectrum of the scattering through just the Kapton™ windows and nitrogen environment could be obtained for each experimental condition. The humidity of the sample environment was controlled by mixing heated streams of saturated and dry nitrogen and measured independently with humidity probe (Vaisala). Sample holders were inserted into an oven environment of 60 °C and 95% relative humidity and allowed to equilibrate for 15 min. The humidity was stepped to 75% RH, 50% RH, 25% RH, dry and back to 95%RH with 17 min steps. Spectra were taken during the last 2 min of each humidity condition.

#### 2.3.4. Imaging

Environmental electron scanning microscope (ESEM) images were acquired with an FEI Quanta 600i ESEM and IR microscopy was acquired using a Thermo IN-10 FTIR microscope.

#### 2.3.5. Diffusion coefficient experiment

The self-diffusion coefficient of water through the membrane was measured by pulsed-field gradient nuclear magnetic resonance (PFG-NMR) spectroscopy with a stimulated echo pulse sequence. Pulse gradient NMR experiments are analyzed using the Stejskal-Tanner-Equation given in Eq. (3).

$$\frac{S}{S_0} = e^{-\gamma^2 G^2 \delta^2 (\Delta - (\delta/3)) D} \quad (3)$$

where  $S$  and  $S_0$  represent the signal amplitude and the signal amplitude at zero gradient,  $\gamma$  is the gyro magnetic ratio,  $G$  is the gradient strength,  $\delta$  is the gradient pulse length,  $\Delta$  is the diffusion time, and  $D$  is the apparent diffusion coefficient. Membrane samples were wound into a cylinder and suspended above saturated potassium chloride salt solution in a 5 mm NMR tube to generate an environment of 84% relative humidity at 30 °C. A pulse gradient stimulated

echo sequence was performed using a Bruker AVANCEIII NMR spectrometer and 400 MHz wide bore Magnex Magnet. Proton diffusion measurements were made using a 5 mm Bruker single-axis DIFF60L Z-diffusion probe. The 90 degree pulse length was of the order of 5.0  $\mu\text{s}$ . Typical parameters at 25 °C were  $G = 0\text{--}128\text{ G cm}^{-1}$ , incremented in 16 steps,  $\delta = 1\text{ ms}$ ,  $\Delta = 6\text{--}700\text{ ms}$ . The Bruker TopSpin software was used for data acquisition and analysis. Multiple diffusion experiments were performed varying the time between pulses ( $\Delta$ ) between 6 and 500 ms with a constant gyromagnetic ratio ( $\gamma$ ) of 4258  $\text{Hz G}^{-1}$  and pulse length ( $\delta$ ) of 1 ms. The maximum gradient strength for each experiment was chosen to produce a full decay of the signal intensity over the length of the experiment. The decay of the signal intensity was plotted against gradient strength for each experiment and was fit to Eq. (1) to determine the diffusion coefficient.

#### 2.3.6. Water uptake

Water uptake experiments were conducted using a dynamic vapor sorption (DVS) apparatus, DVS Advantage (Surface Measurement Systems Ltd). The DVS Advantage was used to measure the mass of water absorbed by the membrane in various humidity environments at 60 °C. The sequence of humidity conditions starts with 4 h of dry nitrogen flow to ensure an accurate initial dry mass. A series of humidity steps follow, where humidified nitrogen is controlled to 20%, 40%, 60%, 80% and 95% relative humidity (RH) for 2 h each. The process is then reversed with 2 h steps at each humidity back down to dry conditions.

Water uptake experiments were also conducted under environmental conditions mimicking the conditions of the small-angle X-ray scattering experiments. In these experiments humidity steps lasted only 17 min and cycled through 95% RH, 75% RH, 50% RH, 25% RH, dry and back to 95% RH nitrogen gas flow.

#### 2.3.7. Ionic conductivity

In-plane conductivity was measured by electrochemical impedance spectroscopy (EIS) using a Bio-Logic VMP3 potentiostat. Data were collected and analyzed using EC Laboratories software. The membrane was held in a four-electrode test cell, with platinum electrodes. Chloride ion conductivity measurements were made while the sample was in a TestEquity H1000 oven that controls temperature and RH. At each RH studied, the temperature was varied from 50 to 90 °C by steps of 10 °C. The relative humidity is measured with a Vaisala humidity sensor. Feedback of this information controls saturated and dry air flow rates as necessary to maintain desired relative humidity throughout the experiment. Samples were allowed to equilibrate to each temperature set-point for 35 min before data was collected.

#### 2.3.8. Counter-ion reaction in air

Infrared spectroscopy was used to monitor the reaction of hydroxide ions with atmospheric  $\text{CO}_2$  to form (bi)carbonate species in the membrane. Quaternized membrane with a chloride counterion was suspended in chloroform and spin coated onto a glass slide. The membrane coated slide was left to dry in atmospheric conditions of temperature and pressure for about a week and a thin membrane (ca. 5  $\mu\text{m}$ ) was peeled from the glass slide. A few drops of water on the slide eased sample removal. The chloride counterions were exchanged to hydroxide ions by immersing the sample in 1 M NaOH solution for 1 day. The membrane in the hydroxide form was rinsed thoroughly with high purity nitrogen gassed DI water and patted with a Kimwipe to absorb excess water. The sample was transferred as quickly as possible to the ATR stage in order to maximize the amount of the (bi)carbonate reaction observed. ATR infrared spectra were collected using a Nexus 470 FT-IR spectroscopy unit. The ATR was equipped with a diamond ATR crystal and a MCT/A detector. 256 scans were averaged to obtain a

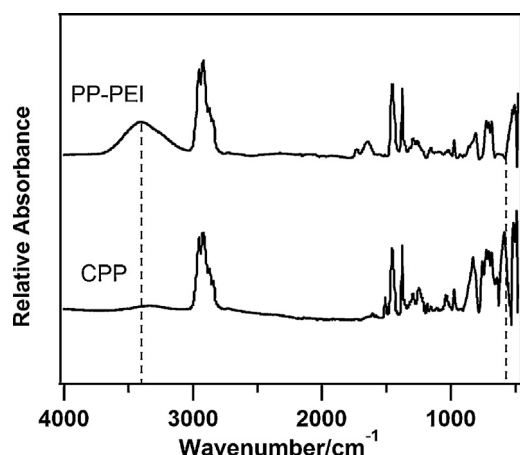


Fig. 2. FT-IR spectra of chlorinated polypropylene starting material (PP-Cl) and the final quaternized product (PP-PEI).

single beam sample spectrum and 10 scans were averaged to obtain a single beam background spectrum. FTIR spectra also were collected for a standard 1 M solution of potassium carbonate and potassium bicarbonate using FTIR spectroscopy. The range of wavenumbers observed for carbonates and bicarbonates were taken as benchmark position to identify the carbonates and bicarbonates peaks during dynamic spectra collection.

### 3. Results and discussion

#### 3.1. Synthesis

Initial attempts to synthesize an AEM from the branched high MW PEI and iodoethane resulted in a hygroscopic material that was obviously impractical due to its solubility in water. When the dried product was exposed to ambient conditions (20 °C, 25% RH), it absorbed enough water to completely dissolve the material. Since a membrane could not be formed from the simple quaternized PEI we reasoned that animating with another polymer followed by quaternization should result in a water stable film. The reaction scheme in Fig. 1 was pursued to form a water insoluble material. To form a film, the product was treated with toluene to form a viscous paste and spread over a Teflon block. After the toluene evaporated, a yellow opaque visually defect free membranes was formed, 20  $\mu\text{m}$  in thickness. The film was stable to water dissolution and was stored until use in water. The membrane ion exchange capacity, as measured by Mohr titration was found to be 0.74(0.04) mequiv.  $\text{mol}^{-1}$ .

#### 3.2. Characterization

##### 3.2.1. Reaction confirmation

The FT-IR (Fig. 2) shows the starting CPP and the resultant quaternized PP-PEI polymer. The reaction is confirmed with the disappearance of the C–Cl stretch at  $550\text{ cm}^{-1}$  and the appearance of a broad peak that grows in at approximately  $3450\text{ cm}^{-1}$  corresponding to the N–C bonds in the ammonium groups and OH stretches of the water absorbed by the sample [9]. The spectra do not show all the same changes as those reported for the linear PEI/CPP materials and it appears that much of the polypropylene starter remains in the polymer.

Fig. 3 shows the  $^1\text{H}$  MAS-NMR spectrum (a) and the  $^{13}\text{C}$  MAS-NMR spectrum (b). Because of the strong proton homonuclear dipolar coupling, the proton spectrum is very broad. The 12 kHz spin rate was insufficient to remove the dipolar couplings in the  $^1\text{H}$  spectrum. The starting materials show well defined peaks for the methylene protons. The peak at  $\delta = 100\text{ ppm}$  of the  $^{13}\text{C}$  spectrum

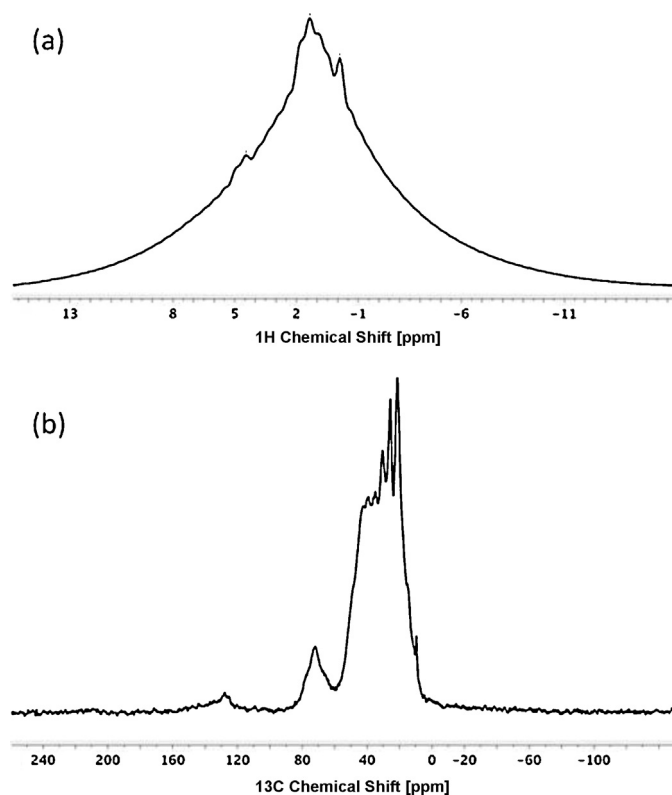


Fig. 3. (a)  $^1\text{H}$  MAS-NMR spectra and (b)  $^{13}\text{C}$  MAS-NMR spectra of the quaternized product.

confirms that the chloride in the starting CPP has fully reacted. The complex peak at ca. 40 ppm is assigned to the methylene carbons in the polymer backbone and the peak at 70 ppm to the methylene carbons adjacent to the quaternary ammonium cations.

##### 3.2.2. Morphology

Wide-angle X-ray scattering (WAXS), not shown, had one peak corresponding to an amorphous polymer structure. The small angle X-ray scattering (SAXS) results are shown in Fig. 4. The scattering pattern had a constant Porod slope between 3.7 and 4.1 in the  $q$ -range of  $0.006\text{--}0.04\text{ \AA}^{-1}$ . In the dried sample this corresponds to a smooth spherical surface on the length scale of 16–105 nm. The reduction the porod slope after humidification is associated with a rougher or less spherical surface. The fact that there are no shoulders or peaks in the scattering pattern shows that there is no ordered structure on the length-scale associated with the  $q$ -range

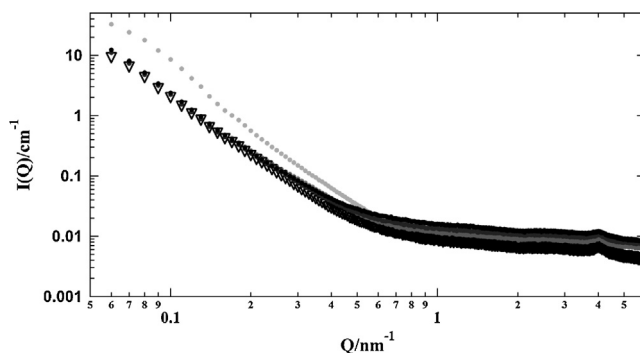
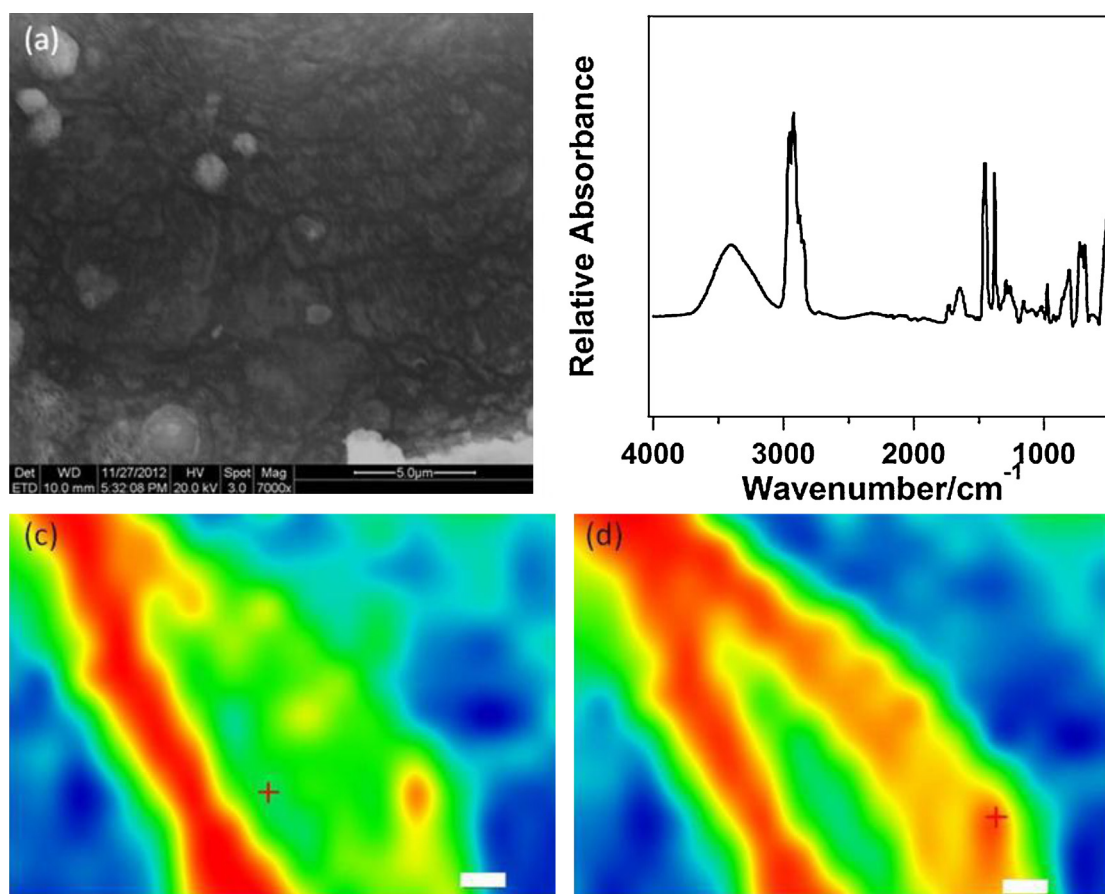


Fig. 4. Small-angle X-ray scattering (SAXS) spectra of PP-PEI membrane with lambda of 16.5, 8.2, 6.6, 4.1 and under dry conditions (black to light gray), and returning to 95% RH (open black triangles).





**Fig. 5.** (a) ESEM image of cast membrane surface, (b) FT-IR spectrum of the quaternized membrane, (c) contour plot of  $3600\text{ cm}^{-1}$  wavenumber intensity with  $100\text{ }\mu\text{m}$  scale bar, (d) contour plot of  $2900\text{ cm}^{-1}$  wavenumber intensity with  $100\text{ }\mu\text{m}$  scale bar.

tested [18]. The material does not appear to phase separate or swell in the size range studied by SAXS.

Relative scattering intensity in organic polymer systems is generally correlated with water content. However, the scattering patterns in Fig. 4 show that the humidified samples have lower intensity relative to the dry sample. This could be attributed to water moving into structure with length scales too large to be observed in the  $q$ -range studied here.

### 3.2.3. Imaging

An ESEM image of the film from the top down, Fig. 5a shows that the material has a heterogeneous appearance with some  $1\text{ }\mu\text{m}$  spherical clusters. This is very similar to the morphology observed by Hong et al. for the materials formed with the linear PEI [9]. When the same material is imaged with a visible microscope, not shown, further heterogeneity is observed. More intriguing is the apparent network of channels that appear to be have a width of  $<0.5\text{ }\mu\text{m}$  and extend across the entire imaged field. These features can be differentiated in the IR. An IR spectrum of this film is shown in Fig. 5b, for reference. In Fig. 5c we show the IR contour plot for the features corresponding to  $3600\text{ cm}^{-1}$  (the OH stretch of water). It indicates that water forms streaks across the film with a width of  $150\text{ }\mu\text{m}$ . When we image the film at  $2900\text{ cm}^{-1}$  (Fig. 5d) corresponding to the methylene chains of the backbone of the polymer we see features again of a width of  $150\text{ }\mu\text{m}$ , but more widespread, suggesting that the polymer may segregate into larger hydrophobic and hydrophilic domains.

### 3.2.4. Diffusion experiment

It is to be expected that anion transport will be mediated by water in this material and so we investigated the self-diffusion of water in these materials by PFG-NMR. Restricted diffusion was probed by a series of NMR experiments with varying times between pulses. The diffusion coefficient for each experiment was plotted vs.  $\Delta$  as shown in Fig. 6. By linear regression of the low range data to zero  $\Delta$ ,  $D_0$  was calculated to be  $1.77 \times 10^{-5}\text{ cm}^2\text{ s}^{-1}$ ,

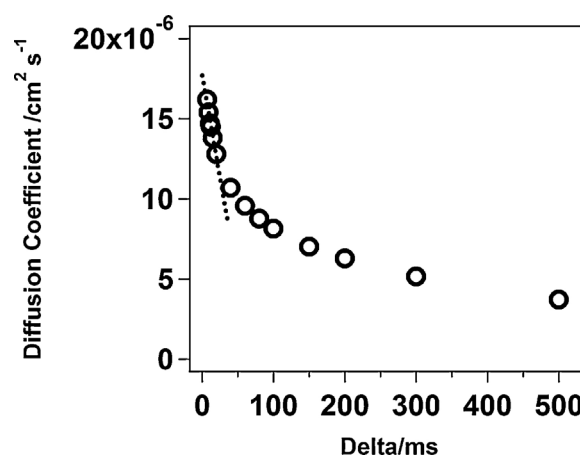


**Fig. 6.** Self-diffusion coefficient versus varying delta ( $\Delta$ ) values where  $\Delta$  is the time between the gradient pulses. Self-diffusion coefficient of water through the PP-PEI membrane calculated from PGSTE results at  $25^\circ\text{C}$  and 80% RH. Dotted line is the linear fit used to calculate a  $D_0$  of  $1.77 \times 10^{-5}\text{ cm}^2\text{ s}^{-1}$ .



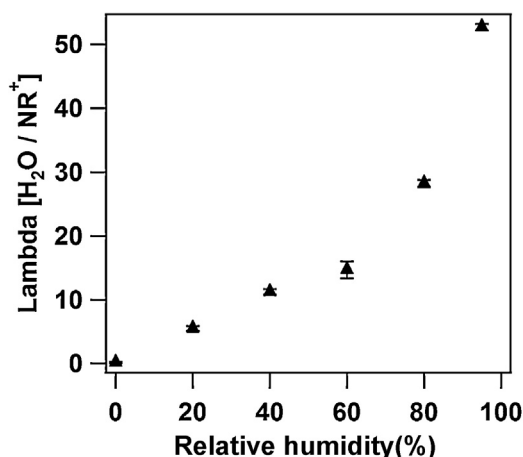


Fig. 7. Lambda versus relative humidity of nitrogen blanket environment for 2 h humidity steps at 60 °C.

close to the value  $2.5 \times 10^{-5} \text{ cm}^2 \text{ s}^{-1}$ , for free water. The maximum measurable diffusion time was  $\Delta = 500 \text{ ms}$  here the diffusion coefficient appears to be approaching the infinite diffusion coefficient and so a simple extrapolation was used to obtain this value,  $D_{\infty} = 3.72 \times 10^{-6} \text{ cm}^2 \text{ s}^{-1}$ , although the diffusion coefficient may continue decreasing slightly beyond this diffusion time. The continued decrease of the diffusion coefficient even at long diffusion times may be a result of transport observed in the much larger feature observed in the ESEM and IR imaging or due to the low resolution of the instrument at very large  $\Delta$ . Nevertheless it appears that there is considerable restriction of the diffusion in the material indicating tortuosity in the anion transport.

### 3.2.5. Water uptake

Water uptake (%) by mass was high as compared to representative AEMs investigated to date [19]. Water uptake reached its high of 70.3 wt% when the sample was at equilibrium with a 95% RH environment, nearly doubling when the relative humidity increased from 80% to 95%. The IEC and water uptake values were used to calculate lambda (Fig. 7). The highest water uptake converted to lambda is 53 water molecules per quaternary ammonium cation. The high lambda values are due to the extreme hydrophilicity of the quaternized PEI which is immobilized within the crosslinked polymer. Interestingly the membranes does not appear to swell dimensionally and so the water is absorbed by the free volume of the quaternized PEI moieties in the material.

### 3.2.6. Ionic conductivity

As expected, the ionic conductivity is highest under the highest temperature and humidity conditions tested (90 °C and 95% RH). The highest chloride ion conductivity observed was  $0.293 \text{ mS cm}^{-1}$ , as shown in Fig. 8. This result is lower than for comparable AEMs. Interestingly, the chloride anion conductivity at 95%RH does not show Arrhenius behavior. When the film is tested at the drier 95%RH condition the chloride conductivity levels off at the higher temperatures. These samples were tested from low to high temperature and so this may be an indication of either cation instability or a significant loss of water. We were unable to measure hydroxide conductivity for these materials under RH cycling conditions as they did not survive the rigorous hydroxide exchange treatment used to obtain and mount films in the fixture in pure hydroxide form.

### 3.2.7. Counter-ion exchange in air

Despite the issues with attempting to make rigorous hydroxide conductivity measurements we were able to demonstrate that

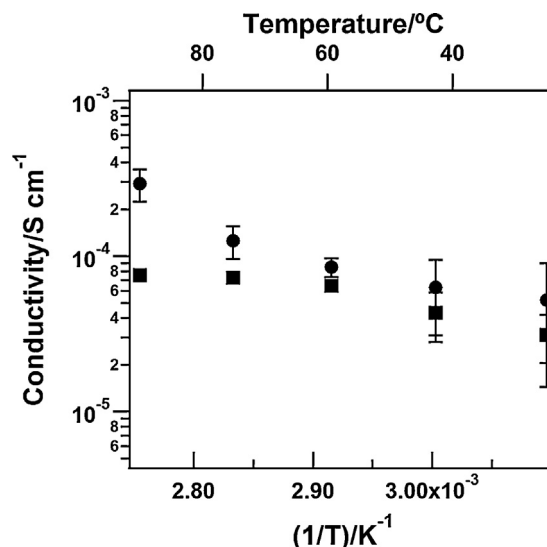


Fig. 8. Chloride ionic conductivity versus temperature at 95% RH (circle) and 80% RH (square).

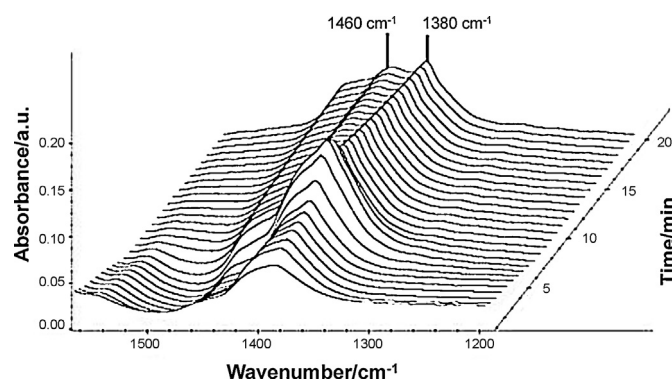


Fig. 9. FT-IR spectra showing increasing C–O stretching at  $1380 \text{ cm}^{-1}$  and  $1460 \text{ cm}^{-1}$  over time due the formation of bicarbonate and carbonate ions respectively.

they reacted with ambient  $\text{CO}_2$ . Time resolved FTIR of the hydroxide film placed on an ATR crystal and exposed to ambient  $\text{CO}_2$  is shown in Figs. 9 and 10. The growth of peaks at  $1460 \text{ cm}^{-1}$  and  $1380 \text{ cm}^{-1}$  assigned to the increasing carbonate and bicarbonate

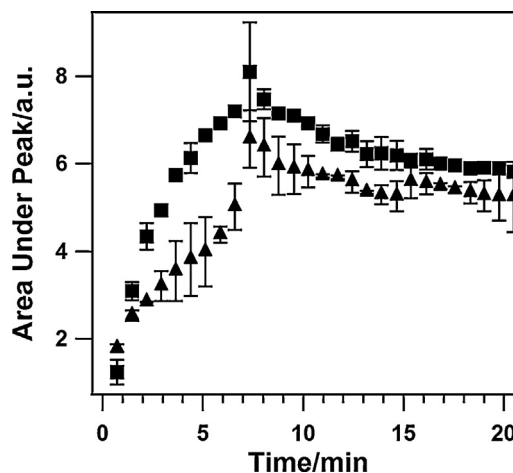


Fig. 10. Calculated area under FT-IR peak at  $1380 \text{ cm}^{-1}$  corresponding to bicarbonate (squares) and under FT-IR peak at  $1460 \text{ cm}^{-1}$  corresponding to carbonate (triangles) versus time.

counter-ions respectively within a hydroxide form membrane exposed to air (Figs. 9 and 10). These peaks were assigned based on comparisons to spectra of standard solutions of potassium carbonate and potassium bicarbonate, although slight differences were observed due to interactions with functional groups in the membrane. A maximum intensity for the two species is reached after 7 min, which presumably corresponds to the consumption of all of the hydroxide. After this time the ratio of carbonate to bicarbonate is maintained as the film slowly reaches equilibrium. A steady-state mixture is reached after 20 min of exposure to atmospheric CO<sub>2</sub> concentrations. These integrated areas are not corrected for the relative absorbance of the two different anions and so it is not implied that the concentration is greatest at 7 min simply that the initial ratio of anions produced eventually relaxes to an equilibrium value.

#### 4. Conclusions

A new randomly crosslinked alkaline exchange membrane was produced through the amination of chlorinated polypropylene (CPP) with polyethyleneimine (PEI) and quaternization with iodoethane. The new material was characterized by FTIR and MAS-NMR. Environmentally controlled small/wide angle X-ray analysis showed relatively featureless amorphous morphology through a full range of humidity environments over the 16–105 nm length scale. Larger scale ordering over >1 μm was observed in ESEM and IR microscope images implying that the water swelling occurs in larger features. However these features swell internally as little dimensional swelling of the material is observed.

Water self diffusion studies indicate rapid short-range diffusion, but heavily restricted diffusion over longer length scales. Temperature and humidity effects on the in-plane chloride ion conductivity were measured using electrochemical impedance spectroscopy (EIS). The highest chloride conductivity observed was 0.29 mS/cm at 90 °C and 95% relative humidity. Infrared spectroscopy was used to monitor the rate of counter-ion exchange from hydroxide to a mixture of carbonate and bicarbonate when exposed to air, which occurred in a time frame of minutes. Unfortunately these materials are too unstable to hydroxide for use in hydroxide exchange membrane fuel cells, but show interesting properties, such as high water uptake with little dimensional swelling, that may make them suitable for use in low temperature carbonate exchange membrane electrochemical systems.

#### Acknowledgements

The authors would like to thank the Army Research Office for support of this research under the MURI program, W911NF-10-1-0520, and for the purchase of the FTIR microscope under the

DURIP program, W911NF-11-1-0462. Use of the Advanced Photon Source was supported by the U.S. Department of Energy, Office of Science, Office of Basic Energy Sciences, under Contract No. DE-AC02-06CH11357. We would also like to thank Dr. Steve J. Hamrock for discussions and for suggesting this idea.

#### References

- [1] W. Cui, J. Kerres, G. Eigenberger, Development and characterization of ion-exchange polymer blend membranes, *Separation and Purification Technology* 14 (1998) 145.
- [2] J.R. Varcoe, R.C.T. Slade, Prospects for alkaline anion-exchange membranes in low temperature fuel cells, *Fuel Cells* 5 (2005) 187.
- [3] X. Wang, J.P. McClure, P.S. Fedkiw, Transport properties of proton- and hydroxide-exchange membranes for fuel cells, *Electrochimica Acta* 79 (2012) 126.
- [4] M. Ali, M. Rakib, S. Laborie, P. Viers, G. Durand, Coupling of bipolar membrane electrodialysis and ammonia stripping for direct treatment of wastewaters containing ammonium nitrate, *Journal of Membrane Science* 244 (2004) 89.
- [5] I. Frenzel, H. Holdik, D. Stamatialis, G. Pourcelly, M. Wessling, Chromic acid recovery by electro-electrodialysis. I. Evaluation of anion-exchange membrane, *Journal of Membrane Science* 261 (2005) 49.
- [6] B. Pivovar, Alkaline membrane fuel cell workshop final report, in: *Proceeding from the Alkaline Membrane Fuel Cell Workshop*, Arlington, VI, 2011.
- [7] G. Merle, M. Wessling, K. Nijmeijer, Anion exchange membranes for alkaline fuel cells: a review, *Journal of Membrane Science* 377 (2011) 1.
- [8] J.-H. Hong, Preparation and characterization of weak-base anion exchange membrane, *Journal of Industrial and Engineering Chemistry* 17 (2011) 208.
- [9] J.-H. Hong, D. Li, H. Wang, Weak-base anion exchange membranes by amination of chlorinated polypropylene with polyethyleneimine at low temperatures, *Journal of Membrane Science* 318 (2008) 441.
- [10] J. Hong, M. Park, S. Hong, B. Kim, Preparation of an anion-exchange membrane by the amination of chlorinated polypropylene and polyethyleneimine at a low temperature and its ion-exchange property, *Journal of Applied Polymer Science* 112 (2009) 830.
- [11] M. Ignatova, S. Voccia, S. Gabriel, B. Gilbert, D. Cossement, R. Jerome, et al., Stainless steel grafting of hyperbranched polymer brushes with an antibacterial activity: synthesis, characterization, and properties, *Langmuir* 25 (2009) 891.
- [12] G. a Pietersz, C.-K. Tang, V. Apostolopoulos, Structure and design of polycationic carriers for gene delivery, *Mini Reviews in Medicinal Chemistry* 6 (2006) 1285–1298.
- [13] B. Gao, X. Zhang, Y. Zhu, Studies on the preparation and antibacterial properties of quaternized polyethyleneimine, *Journal of Biomaterials Science. Polymer Edition* 18 (2007) 531.
- [14] C. Nédéz, J.-L. Ray, Efficient removal of polymerization inhibitors by adsorption on the surface of an optimized alumina, *Langmuir* 15 (1999) 5932.
- [15] J. Yan, M. a. Hickner, Anion exchange membranes by bromination of benzylmethyl-containing poly(sulfone)s: supporting material, *Macromolecules* (2010) 4–7.
- [16] S. Suzuki, H. Muroyama, T. Matsui, K. Eguchi, Influence of CO<sub>2</sub> dissolution into anion exchange membrane on fuel cell performance, *Electrochimica Acta* 88 (2012) 552.
- [17] Y. Liu, J.L. Horan, G.J. Schlichting, B.R. Caire, M.W. Liberatore, S.J. Hamrock, et al., A small-angle X-ray scattering study of the development of morphology in films formed from the 3 M perfluorinated sulfonic acid ionomer, *Macromolecules* 45 (2012) 7495.
- [18] B. Hammouda, NIST, Probing nanoscale structure: SANS Toolbox, 2009.
- [19] P. Mangiagli, C. Ewing, K. Xu, Q. Wang, M. Hickner, Dynamic water uptake of flexible ion-containing polymer network, *Fuel Cells* (2009) 432.